



Rapid High-Frequency Measurements of Electrical Circuits by Using Frequency Mixer and Pseudo-Random Sequences

T. Roinila¹ R. Luhtala¹ T. Salpavaara¹ J. Verho¹ T. Messo² M. Vilkkö¹

¹*Department of Automation Science and Engineering, Tampere University of Technology, Tampere, Finland. E-mail: tomi.roinila@tut.fi*

²*Department of Electrical Engineering, Tampere University of Technology, Tampere, Finland.*

Abstract

Frequency-response measurements at high frequencies have been shown to provide a valuable design tool in various fields of electronics. These measurements are often challenging when using most commercially available measurement tools due to their relatively low maximum sampling frequency and long measurement time. This effectively prevents frequency-response-based low-cost applications where fast and reliable measurements are required. This paper proposes the use of a combined frequency mixer applied with pseudo-random sequences. In this method, the applied pseudo-random excitation is upconverted to high frequencies by the mixer, and once injected into the device being tested, the system response is downconverted to lower frequencies. The method provides a low-cost solution that can be applied for rapid high-frequency measurements by using only modest data-acquisition tools. Experimental results based on a high-frequency resonator are presented and used to demonstrate the effectiveness of the proposed methods.

Keywords: Identification, Frequency measurements, Modeling, Excitation design

1 Introduction

Due to the ever-increasing complexity of electrical circuits and difficulties in forming analytical models, nonparametric frequency-response-measurement methods have become popular in various fields of electronics. Power electronics present a good example of modern applications where nonparametric frequency responses provide a powerful tool in system analysis. The author in (Suntio, 2009) showed that switched-mode power supplies can be fully characterized and controlled by a certain set of frequency responses. The authors in (Meisser et al., 2012) applied impedance-spectra characterization for obtaining the values of parasitic circuit components from practical switched-mode power supplies in order to avoid destructive resonances and to re-

duce electromagnetic radiation. The useful frequency range varied from a few Hertz to up to 100 MHz. Other modern examples where frequency-response measurements at a wide bandwidth provide a valuable design tool include the applications in sensor technology (Salpavaara et al., 2011), in wireless power transfer (Martin et al., 2013) and charging (Khan-ngern and Zenkner, 2014), in sustainable energy production (Roinila et al., 2014), and in nano technology (Roinila et al., 2012).

The prevailing technique to obtain nonparametric frequency responses is to use a network analyzer based on sine sweeps. A set of sinusoidal signals is injected into the device being tested, and the frequency response is then computed by comparing the measured response to the injection. This method usually yields reliable responses but the technique suffers from many

deficiencies of which the most vital one is the length of time required for the measurement. In the case of a single-sinusoid injection the transient period after each frequency change has to be omitted. Depending on the application, the cumulative time for the omitted data may become minutes or even hours. The long measurement time effectively prevents the use of most on-line applications, such as adaptive control and quality assessment, which often require rapid measurements. In the case of a chirp signal (Paavle et al., 2008), or other types of aperiodic broadband excitations such as impulse (Schaefer, 1999) typically used in analyzers, the accuracy is affected by the leakage or uncontrollable spectral energy content of the excitation. Another main issue is that the bandwidth of most commercially available low-cost data-acquisition devices is typically limited to relatively low frequency (usually up to 2 MHz). The option for higher bandwidth (up to 100–200 MHz) significantly increases the price and complexity of the analyzer.

In this paper, a combined frequency mixer is proposed as a low-cost solution for rapid high-frequency measurements. The mixer is a nonlinear circuit that creates new frequencies from two signals that are applied to it. In the mixer, a maximum-length binary sequence (MLBS) (Godfrey, 1991) is mixed by a high-frequency carrier resulting in a high-frequency broadband excitation. The MLBS is a deterministic and periodic signal, and hence, multiple injection periods can be applied through spectral averaging thus increasing the signal-to-noise ratio (SNR). Due to the binary form, the sequence can be simply implemented. The MLBS has the lowest possible peak factor, which means that most of the signal elements are distributed near the minimum and maximum values of the sequence; in other words, the signal does not present large peaks. Thus, the MLBS is well suited for sensitive systems that require small-amplitude perturbation. This is particularly important in online applications where normal system operation needs to be guaranteed during the injection. The mixing procedure does not affect the fundamental properties of the MLBS thus allowing fast and controllable injection into the device being tested. The measured system response is downconverted to lower frequencies by applying similar procedure. As a result, the whole frequency-response-measurement procedure can be performed by a modest, low-frequency data-acquisition unit.

The rest of the paper is organized as follows. Section 2 reviews the theory behind the frequency-response computation, maximum-length binary sequence (MLBS), and combined frequency mixer. Section 3 presents experimental evidence based on a high-frequency resonator. Finally, Section 4 draws conclu-

sions.

2 Methods

Consider a linear time-invariant system for small disturbances. According to basic control theory, this type of system can be fully characterized by its impulse response, which can be transformed into frequency domain and presented by a frequency-response function (Ljung, 1999).

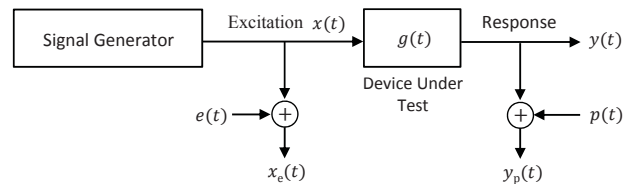


Figure 1: Typical measurement setup.

Fig.1 shows a typical setup where the device being tested, presented by an impulse-response function $g(t)$, is to be identified. The system is perturbed by excitation $x(t)$, which yields the corresponding output response $y(t)$. The measured signals are corrupted with noise, as presented by $e(t)$ and $p(t)$. The measured excitation and output response can now be denoted by $x_e(t)$ and $y_p(t)$. The noises are assumed white noise and are uncorrelated with $x(t)$ and $y(t)$. All of the signals are assumed to be zero mean sequences. The frequency-response function of the device under test can be computed through logarithmic averaging as

$$G_{\log}(j\omega) = \left(\prod_{k=1}^R \frac{Y_{pk}(j\omega)}{X_{ek}(j\omega)} \right)^{1/R} \quad (1)$$

where R denotes the number of injected excitation periods. In this method, the measurements from both input and output sides are segmented and Fourier transformed after which (1) is applied. The method tends to cancel out the effect of uncorrelated noise both from the input and output sides, and hence, provides a good computation algorithm for practical measurements (Pintelon and Schoukens, 2001).

2.1 Maximum-Length Binary Sequence

Pseudo-random binary sequence (PRBS) is a periodic broadband signal based on a sequence of length N . The most commonly used signals are based on maximum-length sequences (maximum-length binary sequence (MLBS)). Such sequences exist for $N = 2^n - 1$, where n is an integer. The reason for their popularity is that they can be generated using feedback shift register circuits (Golomb, 1967).

The power spectrum of an MLBS is given by

$$\Phi_{\text{MLBS}}(q) = \frac{a^2(N+1)}{N^2} \frac{\sin^2(\pi q/N)}{(\pi q/N)^2}, \quad q = \pm 1, \pm 2, \dots \quad (2)$$

where q denotes the sequence number of the spectral line, a is the signal amplitude, and N is the signal length. Fig. 2 shows the form of the power spectrum of an MLBS of length $2^4 - 1 = 15$, generated at 10 Hz. The power spectrum has an envelope and drops to zero at the generation frequency and its harmonics.

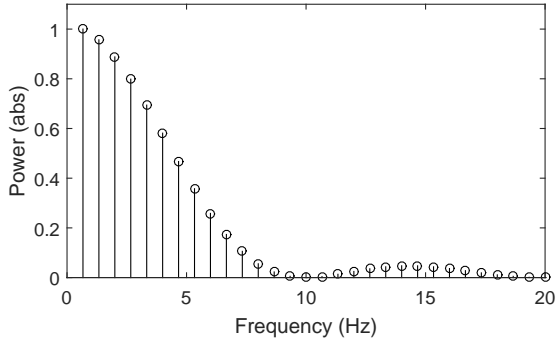


Figure 2: Power spectrum of 15-bit-length MLBS generated at 10 kHz.

The MLBS x has the lowest possible peak factor $|x|_{\text{peak}}/x_{\text{rms}} = 1$ regardless of its length. Hence, the sequence is well suited for sensitive systems which require small-amplitude perturbation. Due to the deterministic nature of the sequence, the signal can be repeated and injected precisely and the SNR can be increased by synchronous averaging of the response periods. The most significant advantage of the MLBS compared to other types of excitations is the binary form of the sequence. This binary form means that the injection can be straightforwardly generated by using a low-cost application, the output of which can only cope with a small number of signal levels.

2.2 Combined Frequency Mixer

A frequency mixer is a nonlinear circuit that creates new frequencies from two signals that are applied to it. In its most common application, two signals (at frequencies ω and α) are applied to a mixer, which then produces new signals at the sum ($\alpha + \omega$) and difference ($\alpha - \omega$) frequencies (Ling et al., 2009). This process is commonly known as heterodyning. In this work, a combined mixer is used to apply first upconversion in order to produce high-frequency excitation into a device under test. The response is then measured and collected by applying downconversion.

The operation principle of the combined frequency mixer is shown in Fig. 3. The excitation signal (with a frequency of ω) is upconverted by the carrier signal originating from a local oscillator of the mixer resulting in the actual excitation $u(t)$. The response signal from the test device is downconverted by applying the same carrier resulting in the output $y(t)$ of the whole process. Due to the upconversions and downconversions, no sophisticated high-frequency data-acquisition methods are required. Thus, the mixer can be operated and the system can be analyzed by a modest measurement tool.

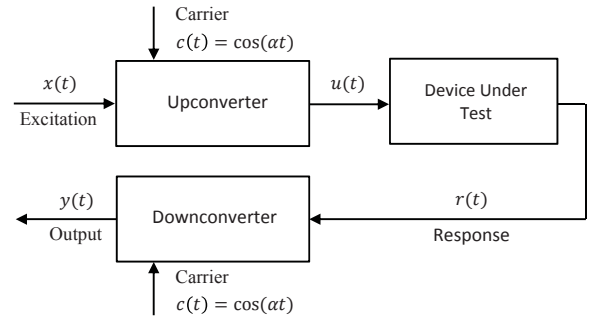


Figure 3: Operation principle of combined frequency mixer.

The upconverted signal $u(t)$ can be denoted as

$$u(t) = x(t)\cos(\alpha t) = \frac{e^{j\alpha t} - e^{-j\alpha t}}{2}x(t) \quad (3)$$

where α is the frequency of the carrier. The signal can be represented in the frequency domain as

$$U(\omega) = \frac{1}{2}X(\omega - \alpha) + \frac{1}{2}X(\omega + \alpha) \quad (4)$$

where $X(\omega)$ denotes the Fourier transform of $x(t)$. Fig. 4 shows an example of the upconversion process. The MLBS shown in Fig. 2 is mixed with a 50 Hz carrier. As the figure shows, the upconverted sequence is divided into two frequency bands, both having half of the total energy from the original MLBS.

The downconverter of the mixer applies the same carrier as the upconverter. Assuming there is no test device at this point the output signal of the upconverter $u(t)$ can be used as an input signal of the downconverter. The downconverted signal can be denoted as

$$y(t) = u(t)\cos(\alpha t) = x(t)\cos^2(\alpha t) \quad (5)$$

Applying the Fourier transform, (5) can be represented in the frequency domain as

$$Y(\omega) = \frac{1}{2}F(\omega) + \frac{1}{4}F(\omega - 2\alpha) + \frac{1}{4}F(\omega + 2\alpha) \quad (6)$$

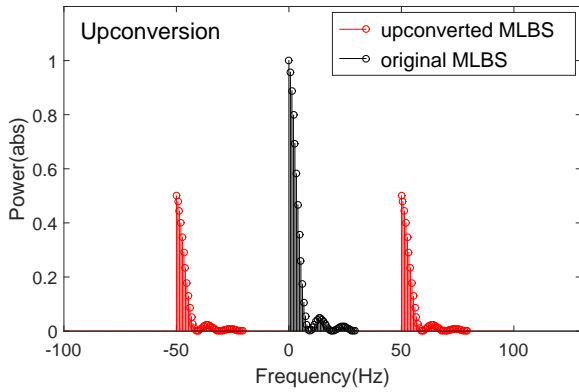


Figure 4: MLBS with 50 Hz upconversion.

The equation shows that the translated signal undergoes a 6 dB loss (a 50 percent reduction) at ω , and 12 dB loss (a 75 percent reduction) at the sideband frequencies as dictated by the factors $1/2$ and $1/4$.

The input signal $x(t)$ of the downconverter has the sum and difference frequencies at $\omega + \alpha$ and $\omega - \alpha$, respectively. Because the same carrier is applied to the downconverter, its output $y(t)$ has the following frequency components:

- 1) $\omega + \alpha + \alpha = \omega + 2\alpha$
- 2) $\omega + \alpha - \alpha = \omega$
- 3) $\omega - \alpha - \alpha = \omega - 2\alpha$

Fig. 5 shows an example of the downconversion process. The upconverted MLBS from Fig. 4 is mixed with the same 50 Hz carrier. Now the downconverted sequence is divided into three frequency bands, each having energy content as stated by (6).

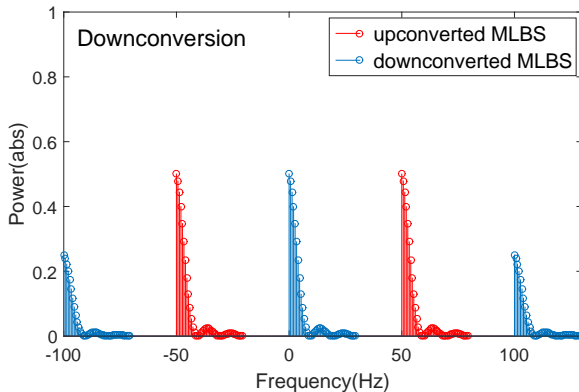


Figure 5: MLBS with 50 Hz downconversion.

The form of the modulation is known as double sideband modulation because the excitation is transformed

to a frequency range above and below the carrier signal. To eliminate either the upper or lower sideband, another form of modulation known as quadrature modulation can be employed. A quadrature modulator mixes the excitation with two mixing signals. Both mixing signals operate at the same frequency, but are shifted in phase by 90 degrees relative to one another. The excitation also is modified so as to have two separate signals: the original one and a 90-degree phase-shifted version.

For quadrature modulation, the two carriers can be given by sine and cosine components as $c_1 = \cos(\alpha t)$ and $c_2 = \sin(\alpha t)$. The excitation $u(t)$ is formed by mixing the original injection with the cosine component and subtracting the mix of phase-shifted version of the original injection and the sine component from it. Hence, $u(t)$ can be given as

$$\begin{aligned} u(t) &= [\cos(\omega t)\cos(\alpha t)] - [\sin(\omega t)\sin(\alpha t)] \\ &= \left[\frac{1}{2}\cos(\omega t + \alpha t) + \frac{1}{2}\cos(\omega t - \alpha t) \right] \\ &\quad - \left[\frac{1}{2}\cos(\omega t - \alpha t) - \frac{1}{2}\cos(\omega t + \alpha t) \right] \end{aligned} \quad (7)$$

Now, (7) reduces to $\cos(\omega t + \alpha t)$, the upper sideband only. For the downconverter, the sign of the operator on the left-hand side in (7) is changed, resulting in $\cos(\omega t - \alpha t)$.

3 Experimental Measurements

3.1 System Setup

The presented methods are applied to an inductively coupled passive resonance sensor based on an RLC resonance circuit shown in Fig. 6, where M_1 , M_2 and M_3 denote the mutual inductances. The measurand can be linked to the inductance or the capacitance of the resonating circuit, thus altering the circuit's resonance frequency. Alternatively, the measurand can be linked to the losses. The inductively coupled passive resonance sensor has been tested in many applications. The pressure sensors that utilize alternating capacitor are one of the most common applications (Chen et al., 2010). The measurement method can also be used for detecting chemical (Potyrailo and Surman, 2013) and biological variables (Mannoor et al., 2012). By using a voltage-dependent capacitor, this concept can be modified to measure biopotential voltages (Riistama et al., 2010) and pH (Horton et al., 2011). The resonance frequency of the RLC circuit is often prone to other environmental variables besides the measurand. This can be partially compensated by having multiple sensors that can measure more than one variable.

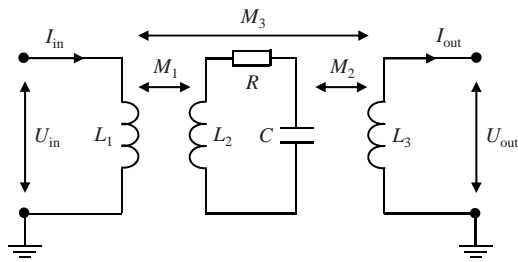


Figure 6: RLC resonance circuit.

The resonance circuit is inductively sensed by measuring a reader coil. Making a frequency sweep over the expected resonance frequency is one of the most common ways to make the actual measurement; this can be done with an impedance analyzer or with another device that measures the reflected parameters of the reader coil by doing frequency sweeps. The speed and frequency range of the sweep can limit the possible applications. The ability to perform fast frequency sweeps at different frequency ranges is important particularly if multiple passive resonance sensors are simultaneously used as an array or matrix.

The objective of the experiment is to measure the frequency response from input voltage to output voltage of a prototype resonance circuit conceptually shown in Fig. 6. The actual set-up for the measurement is shown in Fig. 7. The MLBS perturbation is generated by a signal generator, after which the injection is upconverted by the mixer. The output response of the target is downconverted, after which the data is sampled by a data-acquisition unit. The data is then processed, and the frequency response is computed.

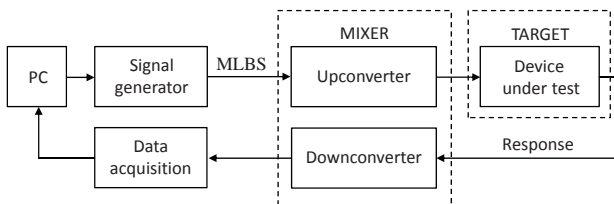


Figure 7: Measurement setup.

The implemented mixer consists of a quadrature up-converter, quadrature downconverter and the associated local oscillators, filters and control electronics. These initially allow shifting the MLBS injection to the frequency range of interest (center frequency 0 – 200 MHz) and then back to baseband so that relatively cheap MLBS hardware can be used. The upconverter output has 50 Ω impedance, while the downconverter has a high-impedance input with roughly 16 pF capacitance. Instead of the normal square wave mixers, the mixers are implemented as analog multipliers in order

to simplify the resulting spectrum.

3.2 Experimental Results

The applied MLBS was produced by a 10-bit-length shift register, and generated at 5 MHz. The resonance frequency of the target circuit was known to be approximately 48 MHz. Hence, the carriers of the mixer were set to 46 MHz resulting in a good spectral energy content around the frequency band of interest. In the case of unknown circuit elements, the frequencies of the carriers can be swept over a large frequency range for obtaining a specific frequency range for the actual identification. Fig. 8 shows a sample of the applied MLBS injection before upconversion in the time domain (± 0.5 V), and its normalized spectral energy.

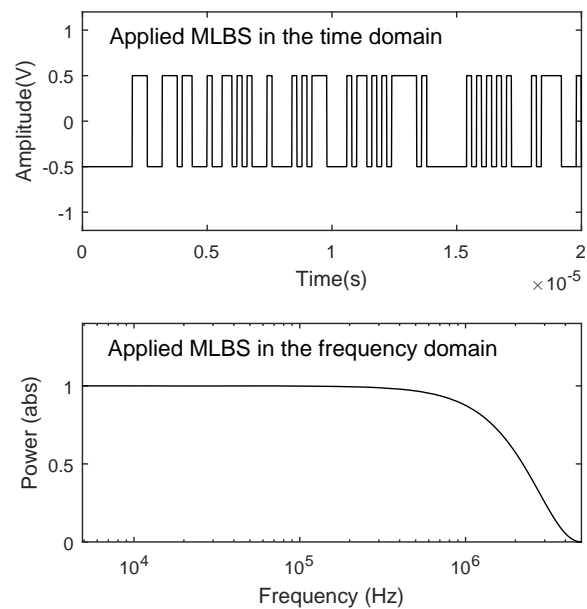


Figure 8: Sample of the applied MLBS injection in the time domain, and the spectral energy content of the sequence.

The MLBS was injected with four periods through the mixer and applied as input voltage to the resonance circuit. The sensed output voltage was down-converted and sampled at 100 kHz. The data was then segmented according to the period length of the MLBS and Fourier transformed (the first period was neglected due to transient), after which (1) was applied. Fig. 9 shows a sample of the computed Bode plot of the resonance circuit. The frequency response was also measured by sine sweeps for comparison (reference). As the figure shows, the curves obtained by the MLBS

very accurately follow the reference in a wide range of frequencies, showing only a few degrees of error below the resonance frequency (47.52 MHz). The measurement time using the MLBS was less than one second.

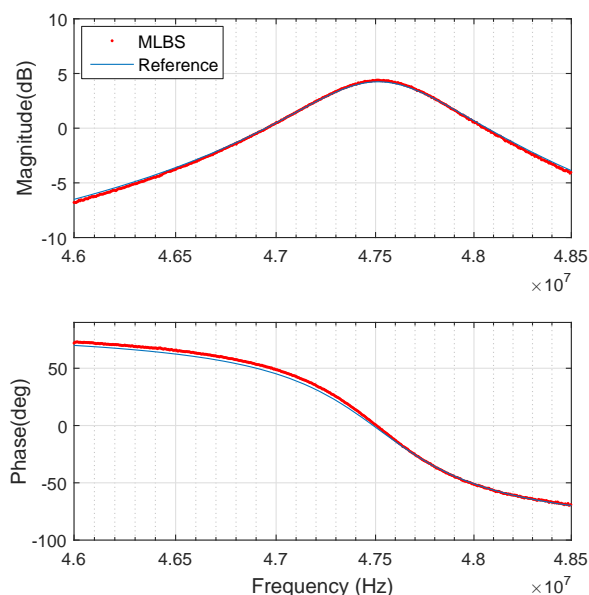


Figure 9: Output impedance of the resonator using MLBS and sine sweep (reference).

4 Conclusions

This paper has presented a nonparametric frequency-response-measurement method for high frequencies (30 MHz and above) based on a combined frequency mixer and maximum-length binary sequence (MLBS). In this method, the applied perturbation is upconverted to higher frequencies, injected into device under test, and the system response is then downconverted into lower frequencies. Due to mixing procedures, the measurement can be performed by applying only modest measurement tools operating at a low sampling frequency. With the exception of the locations of the frequency harmonics and the level of spectral energy, the properties of the MLBS are not affected by the mixing procedures. Due to low peak factor of the MLBS, the amplitude of the injection can be kept relatively small compared to other types of excitations, thus guaranteeing normal system operation during the identification. The method can be used in various fields of electronics, and it is particularly well suited for online applications such as adaptive control and quality assessment, where rapid measurements are required.

Acknowledgements

This work is supported by the Academy of Finland.

References

- Chen, P.-J., Saati, S., Varma, R., Humayun, M., and Tai, Y.-C. Wireless intraocular pressure sensing using microfabricated minimally invasive flexible-coiled LC sensor implant. *Journal of Microelectromechanical Systems*, 2010. 19(4):721–734. doi:[10.1109/JMEMS.2010.2049825](https://doi.org/10.1109/JMEMS.2010.2049825).
- Godfrey, K. R. Introduction to binary signals used in system identification. In *Proc. International Conference on Control*. pages 161–166, 1991.
- Golomb, S. *Shift Register Sequences*. San Francisco, Holden-Day, 1967.
- Horton, B., Schweitzer, S., DeRouin, A., and Ong, K. A varactor-based, inductively coupled wireless ph sensor. *IEEE Sensors Journal*, 2011. 11:1061–1066. doi:[10.1109/JSEN.2010.2062503](https://doi.org/10.1109/JSEN.2010.2062503).
- Khan-ngern, W. and Zenkner, H. Wireless power charging on electric vehicles. In *Proc. of the International Electrical Engineering Congress*. pages 1–4, 2014. doi:[10.1109/ieecon.2014.6925964](https://doi.org/10.1109/ieecon.2014.6925964).
- Ling, W., Sotiriadis, P., and Adams, R. Mixed signal frequency mixers with intermodulation product cancellation. *IEEE International Symposium on Circuits and Systems*, 2009. pages 2105–2108. doi:[10.1109/ISCAS.2009.5118210](https://doi.org/10.1109/ISCAS.2009.5118210).
- Ljung, L. *System Identification-Theory for the User*. Prentice Hall PTR, USA, 1999.
- Mannoor, M., Tao, H., Clayton, J., Sengupta, A., Kaplan, D., Naik, R., Verma, N., Omenetto, F., and McAlpine, M. Graphene-based wireless bacteria detection on tooth enamel. *Nature Communications*, 2012. 3:1–8. doi:[10.1038/ncomms1767](https://doi.org/10.1038/ncomms1767).
- Martin, D., Nam, I., Siegers, J., and Santi, E. Wide bandwidth three-phase impedance identification using existing power electronics inverter. In *Proc. The Applied Power Electronics Conference and Exposition*. pages 334–341, 2013. doi:[10.1109/apec.2013.6520230](https://doi.org/10.1109/apec.2013.6520230).
- Meisser, M., Hhre, K., and Kling, R. Impedance characterization of high frequency power electronic circuits. In *International Conference on Power Electronics, Machines and Drives*. pages 1–6, 2012. doi:[10.1049/cp.2012.0240](https://doi.org/10.1049/cp.2012.0240).

- Paavle, T., Min, M., and Parve, T. Using of chirp excitation for bioimpedance estimation: Theoretical aspects and modeling. In *Proc. 11th International Biennial Baltic Electronics Conference*. pages 325–328, 2008. doi:[10.1109/bec.2008.4657546](https://doi.org/10.1109/bec.2008.4657546).
- Pintelon, R. and Schoukens, J. *System Identification - A Frequency Domain Approach*. The Institute of Electrical and Electronics Engineers, Inc. New York, 2001. doi:[10.1002/0471723134](https://doi.org/10.1002/0471723134).
- Potyrailo, R. and Surman, C. A passive radio-frequency identification (RFID) gas sensor with self-correction against fluctuations of ambient temperature. *Sensors and Actuators B: Chemical*, 2013. 185:587–593. doi:[10.1016/j.snb.2013.04.107](https://doi.org/10.1016/j.snb.2013.04.107).
- Riistama, J., Aittokallio, E., Verho, J., and Lekkala, J. Totally passive wireless biopotential measurement sensor by utilizing inductively coupled resonance circuits. *Sensors and Actuators A: Physical*, 2010. 157(2):313–321. doi:[10.1016/j.sna.2009.11.038](https://doi.org/10.1016/j.sna.2009.11.038).
- Roinila, T., Vilkkö, M., and Sun, J. Online grid impedance measurement using discrete-interval binary sequence injection. *IEEE Journal of Emerging and Selected Topics in Power Electronics*, 2014. 2:985–993. doi:[10.1109/JESTPE.2014.2357494](https://doi.org/10.1109/JESTPE.2014.2357494).
- Roinila, T., Yu, X., Gao, A., Li, T., Verho, J., Vilkkö, M., Kallio, P., Wangy, Y., and Lekkala, J. Characterizing leakage current in silicon nanowire-based field-effect transistors by applying pseudo-random sequences. In *Proc. International Conference on Manipulation, Manufacturing and Measurement on the Nanoscale*. 2012. doi:[10.1109/3m-nano.2012.6472995](https://doi.org/10.1109/3m-nano.2012.6472995). 5 pages.
- Salpavaara, T., Verho, J., Kumpulainen, P., and Lekkala, J. Readout methods for an inductively coupled resonance sensor used in pressure garment application. *Sensors and Actuators A: Physical*, 2011. 172(1):109–116. doi:[10.1016/j.sna.2011.02.051](https://doi.org/10.1016/j.sna.2011.02.051).
- Schaefer, W. Understanding impulse bandwidth specifications of EMI receivers. In *Proc. IEEE International Symposium on Electromagnetic Compatibility*. pages 958–961, 1999. doi:[10.1109/isehc.1999.810195](https://doi.org/10.1109/isehc.1999.810195).
- Suntio, T. *Dynamic Profile of Switched-Mode Converter*. Wiley-VCH Verlag GmbH and Co. KGaA, Weinheim, 2009. doi:[10.1002/9783527626014](https://doi.org/10.1002/9783527626014).